Adsorption and interaction of Sb on Si(001) studied by scanning tunneling microscopy and core-level photoemission

D. H. Rich, F. M. Leibsle, A. Samsavar, E. S. Hirschorn, T. Miller, and T.-C. Chiang
Department of Physics, University of Illinois at Urbana-Champaign, 1110 West Green Street, Urbana, Illinois 61801
and Materials Research Laboratory, University of Illinois at Urbana-Champaign, 104 South Goodwin Avenue, Urbana, Illinois 61801
(Received 6 February 1989)

Scanning tunneling microscopy (STM) and synchrotron photoemission were used to analyze the Sb/Si(001) interface formation for submonolayer and saturation coverages. The surface-shifted core-level component observed in photoemission for Si(001)-(2×1) was suppressed with the adsorption of Sb. Constant-current STM images which were taken for different sample bias conditions show changes in the spatial distribution of the occupied and unoccupied states derived from the Si-dimer dangling bonds upon Sb adsorption. These observations are interpreted in terms of the formation of Sb—Si bonds and the resulting modifications in the surface electronic properties.

I. INTRODUCTION

The interaction of group-V adsorbates such as Sb and As with the Si and Ge crystal surfaces has been the subject of much research in recent years. Important benefits gleaned from this research entail an improvement of the quality of III-V–compound epitaxial growth on these group-IV substrates and a more precise control over doping processes. Scanning tunneling microscopy (STM) has proven to be an invaluable tool in determining the local atomic structure of clean semiconductor surfaces and, more recently, adsorbate-covered semiconductor surfaces.[1] Synchrotron photoemission from the core levels can provide additional detailed information about the interaction between the adsorbate and substrate.[2] Since atoms in different chemical environments show different chemical shifts in photoemission, the interaction can be deduced from the evolution of the various chemically shifted core-level components during the interface formation. This study employs both STM and synchrotron photoemission techniques to examine the Sb/Si(001) system.

In the first part of this study, large-area constant-current STM images were taken to assess the quality of the starting clean Si(001)-(2×1) surface. Currently there is much interest in examining the domain structure of the Si(001) surface, which may have bearing on the antiphase disorder during the growth of III-V materials. Alerhand, Vanderbilt, Meade, and Joannopoulos showed that the spontaneous formation of domains on Si(001) is a natural consequence of the anisotropy in the intrinsic surface stress caused by the dimerization.[3] There have also been discussions and theoretical suggestions concerning the spontaneous formation of defects on the surface.[4]

In the second part of this study, the changes in the surface-electronic structure and topography of Si(001) upon Sb adsorption are examined for various coverages. The Sb adsorption suppresses the surface shift for the Si $2p$ core level in photoemission, and the STM results show interesting changes in the spatial distribution of the occupied and unoccupied surface electronic states. High-energy electron diffraction (HEED) is employed to further assess changes in the long-range periodicity of the system. These results lead to a model describing the Sb interaction with the Si dimers.

II. EXPERIMENTAL DETAILS

The STM experiments were performed in a vacuum chamber equipped with HEED and molecular-beam-epitaxy (MBE) capabilities. The base pressure of the chamber was less than 1×10^{-10} Torr. The STM used in this study is fairly similar to that described by Demuth, Hamers, Tromp, and Welland in that the sample is mounted on a lever which allows the sample to be moved into STM, HEED, MBE, and sputtering positions.[5] Tips were constructed by electrochemical etching of tungsten wire in a $2M$ NaOH solution followed by electroplating the tip with a thin layer of gold.[6]

The photoemission experiments were conducted at the Synchrotron Radiation Center at Stoughton, WI of the University of Wisconsin–Madison using the 1-GeV storage ring Aladdin. The University of Illinois extended-range grasshopper monochromator was used to select photon energies for the experiments. An angle-integrating hemispherical analyzer was used for collecting and analyzing the photoelectrons. The Si $2p$ core-level spectra were taken with a photon energy of 150 eV for a high degree of surface sensitivity. The overall instrumental resolution was ~0.15 eV. The photoemission chamber also had the capabilities of HEED, Auger spectroscopy, and MBE.

All samples used in this study were n-type Si(001), having a resistivity of 10 Ω cm, and were cut from a commercial wafer stock. The samples were cleaned in the vacuum chamber by Ohmic heating to about 1100 °C for 10 s;

 ©1989 The American Physical Society

based on our experience, this procedure produces the sharpest HEED pattern with the minimum amount of background (better than that produced by sputtering and annealing). The Sb overlayers were prepared by evaporation with a rate in the range of 1–10 monolayers (ML) per minute. In this paper 1 ML of Sb is defined as 6.8×10^{14} atoms/cm^2, which is the site density for an unreconstructed Si(001) surface. The sample temperature during evaporation was maintained between 320 and 370 °C. Upon exposure to the Sb beam, the sticking coefficient was found to approach zero once the coverage approached to saturation limit of approximately 1 ML.[7,8] After the Sb exposure, the surface was further annealed for 1 min at the same temperature, and allowed to cool to nearly room temperature before the measurements.

III. RESULTS AND DISCUSSION

A. HEED results

HEED was performed only after the STM and photoemission measurements so as to avoid possible carbidization of the surface. The clean Si(001) surface showed a sharp two-domain (2×1) pattern, with an occasional small mixture of $p(2\times2)$ seen in some samples. Upon Sb adsorption, the half-order spots of the clean surface gradually diminished and the background became higher for increasing coverages. At saturation, the half-order spots were weak but still visible on top of a high background. The increase in background indicated that the system became disordered upon Sb adsorption.

B. Dimers, steps, and domains on clean Si(001)-(2×1)

The STM topographs of clean Si(001)-(2×1) were taken with a constant tunneling current of 1 nA for a variety of sample bias voltages ranging from −3 to +3 V. Figures 1 and 2 show typical "raw" images covering 640×640- and 260×260-Å^2 areas, respectively, taken with a −1.3-V bias. The images are somewhat distorted due to thermal drift of the sample and nonlinearity and creep of the piezoelectric transducers. The latter effect causes more apparent distortion near the bottom of each image because the left-to-right rastering pattern of the image begins at the bottom. Due to the presence of many atomic steps in a typical large-area scan, the overall height variation in an image is much larger than the atomic corrugation in a flat terrace. If the grey scale of the image is shown based on the actual height variation, the atomic corrugation would be lost in the picture. To overcome this problem, the images in Figs. 1 and 2 were taken with an ac-coupling scheme, which filters out the long-wavelength components in the picture. This tends to emphasize the local height variation and provides a shadowing effect, so the image appears to be a landscape being illuminated with light from the left above the horizon.

The images show many orthogonally oriented domains of parallel stripes. Each stripe represents a row of Si dimers with the direction of dimerization perpendicular to the stripe, as previously reported by Hamers, Tromp, and Demuth.[9] Each dimer occupies an area of 7.68×3.84 Å^2. The dimer rows are occasionally interrupted by vacancy-type defects. Within a given domain the density of defect sites is typically 5–10 %, and this is consistent with the results obtained by Hamers, Tromp, and Demuth,[9] who thought that the defects were intrinsic and not an artifact due to the sample preparation procedure. Our results are in agreement with this interpretation in that for all samples prepared we always find similar defect densities, and for Si(111)-(7×7) prepared under similar conditions the defect density is much lower. With a larger magnification of the topograph, the dimers can be seen to be either nonbuckled (symmetric) or buckled (asymmetric). The buckled dimers are mainly found near domain boundaries and defects. Neighboring dimers in a row of buckled dimers have opposite directions of buck-

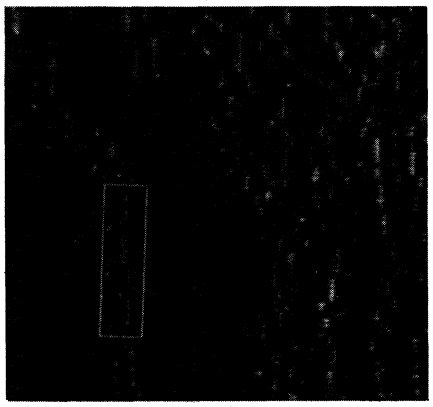

FIG. 1. Constant-current STM image of a 640×640-Å^2 region of clean Si(001)-(2×1) with sample bias of −1.3 V. Examples of S_A- and S_B-type steps are surrounded by white and black rectangles, respectively.

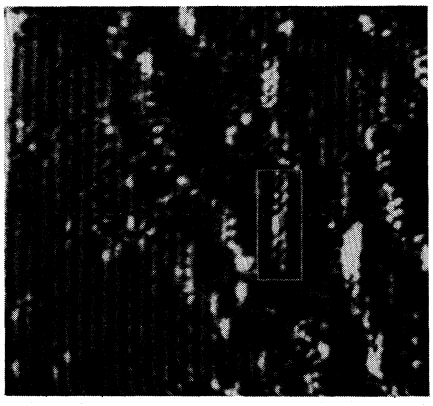

FIG. 2. Constant-current STM image of a 260×260-Å^2 region of clean Si(001)-(2×1) with sample bias of −1.3 V. A white rectangle surrounds an S_A-type step.

ling; consequently, the row appears as a zigzag stripe in the image.[9]

The topograph in Fig. 1 further reveals a large variation in the domain size and shape that can occur for Si(001)-(2×1). The second large domain from the left with vertical dimer rows extends beyond the entire 640-Å height of the picture, while some of the domains at the right of Fig. 1 are quite small. Many atomic steps separating two neighboring orthogonally oriented domains are seen. Steps for which the direction of dimerization on the upper terrace is normal and parallel to the step edge are labeled S_A and S_B, respectively, following the notation of Kroemer.[10] The white and black rectangles drawn in Figs. 1 and 2 represent examples of S_A and S_B steps, respectively. A careful inspection of Fig. 1 and other topographs shows that S_A steps occur more frequently than S_B steps with a ratio $S_A/S_B \approx 3$. This result is consistent with a total-energy calculation performed by Chadi based on a semiempirical tight-binding method, which showed the S_A to be energetically more favorable than the S_B steps.[11] A noticeable buckling of the dimers near a step edge is seen, e.g., the area represented by the rectangle in Fig. 2, which shows a characteristic enhancement in resolution of neighboring dimers in a row relative to dimer rows located away from steps. Similar steps have been seen for smaller regions on the Si(001), vicinal Si(001), and vicinal Ge(001) surfaces.[9,12,13] Using an elastic-continuum theory to calculate the domain-wall energy, Alerhand, Vanderbilt, Meade, and Joannopoulos concluded that for a model of Si(001) consisting of only long striped domains separated by monatomic steps, the domain width is between 300 and 1000 Å.[3] Clearly, the actual scenario is more complicated, as evidenced by the large variation in the domain size and presence of both S_A and S_B steps seen in Fig. 1. The actual domain morphology is governed by the interplay of the energy required for step formation and the configurational entropy associated with the formation of terraces varying in size and shape. For comparison, Aspnes and Ihm have used thermodynamic arguments to show that only biatomic steps are favorable for vicinal Si(001)-(2×1).[14]

Photoemission from the Si 2*p* core level of the clean Si(001)-(2×1) surface has been described before;[2,15–17] a surface-sensitive spectrum is included in Fig. 3 for reference purposes. The decomposition of the spectrum into the bulk (*B*) and surface (*S*) contributions and the overall fit to the data are shown by the various curves. The details of this line-shape analysis can be found in earlier publications.[15–18] Previous studies have identified the surface emission to be derived from the surface dimer atoms, and the surface core-level binding-energy shift has been attributed to the reduced coordination for the surface atoms (threefold coordinated with a dangling bond) relative to the bulk atoms (fourfold coordinated). The principal mechanism leading to the −0.5-eV surface shift is an increased electron localization about the dimer atoms resulting from the unsaturated dangling-bond orbital. The total surface emission has been determined to be about 0.9 ML; namely, the number of surface atoms with a dangling bond is 0.9 ML.[16] The approximate 10% departure from the ideal value of 1 ML is consistent with the defect density measured here.

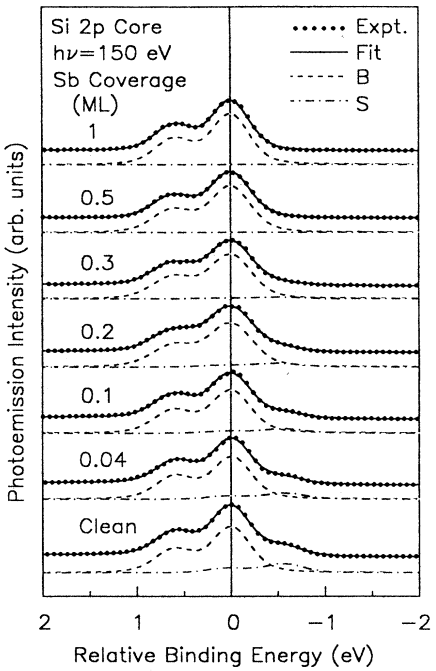

FIG. 3. Si 2*p* core-level spectra (dots) taken with a photon energy of 150 eV for the clean Si(001)-(2×1) and Sb-covered Si(001) surfaces. The Sb coverages are indicated. The solid curves are the result of the fit to the data. The decomposition of the spectra into the bulk (*B*) and surface (*S*) contributions are shown by the dashed and dashed-dotted curves, respectively. The relative binding-energy scale is referred to the Si $2p_{3/2}$ core-level component of the bulk contribution.

C. Adsorption and interaction of Sb on Si(001)

1. Photoemission results

The photoemission spectra of the Si 2*p* core level for various Sb coverages are shown in Fig. 3. The binding energy of the spectra are aligned with respect to the bulk Si $2p_{3/2}$ components for each Sb coverage. The main effect of the adsorption of Sb is the suppression of the surface shift. This behavior is similar to that reported previously for the adsorption of In, Sn, and Ag on Si(001).[15,17,19] The simplest interpretation is that the dimer dangling bonds, which are the cause for the surface shift, become saturated after bonding to the Sb. The surface atoms become fourfold coordinated after the chemisorption bond is formed, resulting in a bulklike bonding environment; hence the surface shift is suppressed. Since the electronegativities of Si and Sb are similar, the Sb—Si bond should be nearly covalent and hence electronically similar to the Si—Si bond.[2]

The photoemission intensity of the surface-shifted component relative to the total intensity (i.e., the *S*-component weight) is shown in Fig. 4 as a function of Sb

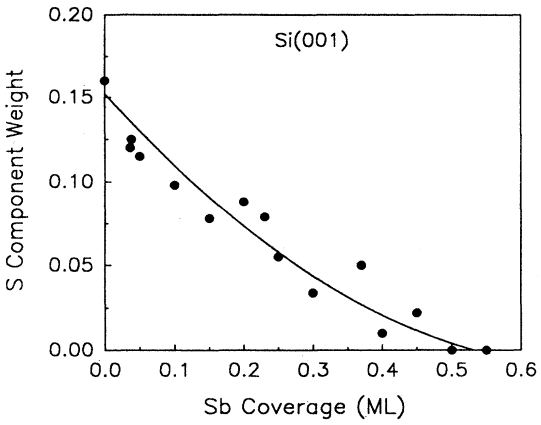

FIG. 4. The weights (fraction of total intensity) of the surface (S) component obtained from spectra like those shown in Fig. 3. The solid curve represents a quadratic fit to the data and serves as a guide for the eye.

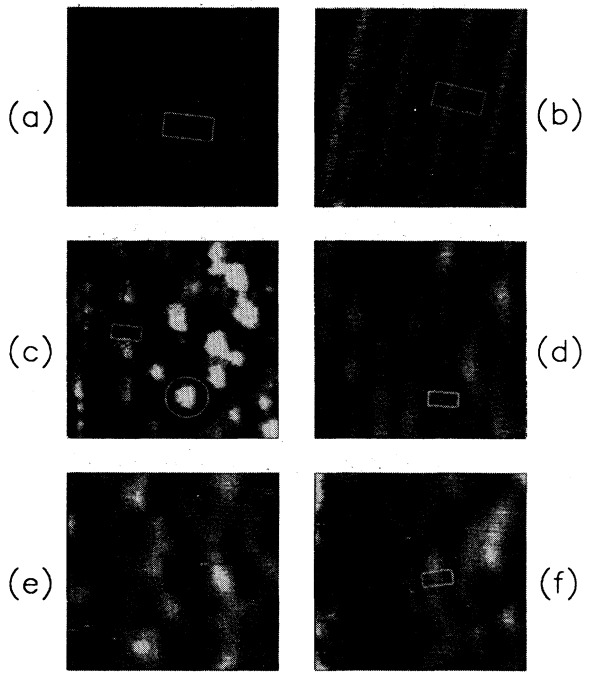

FIG. 5. Constant-current STM images of Si(001) and Sb-covered Si(001). Dark and bright areas represent depressions and protrusions, respectively. The Sb coverages and sample bias voltages are (a) clean, −2.0 V; (b) clean, +1.3 V; (c) 0.3 ML, −2.4 V; (d) 0.3 ML, +2.4 V; (e) 1 ML, −2.5 V; (f) 1 ML, +2.8 V. The rectangles indicate a (2×1) unit cell and circles outline typical bumps due to the Sb-induced disorder.

coverage, which should reflect the number of dimer dangling bonds left intact. A quadratic curve is fitted through the data to serve as a smooth guide. At about 0.5-ML coverage, this weight becomes zero, meaning all dangling bonds have been saturated. The average number of Si atoms which have been converted to have a bulklike binding energy in the presence of an Sb adatom can be calculated based on these data; it depends on the Sb coverage and decreases from approximately three to two for increasing coverages between 0 and 0.5 ML. The chemical valence of Sb is nominally 3, and Sb possesses oxidation states of ±3 and +5 in a variety of compounds. In III-V compounds involving Sb, the coordination number is 4. Therefore, the Sb adatoms can assume various adsorbate-to-substrate coordination numbers depending on the details of the bonding configurations.[2,15,17,19]

2. *STM results*

The Si(001) surface shows considerable disorder after Sb adsorption as revealed by both HEED and STM. The structure of the atomic steps can no longer be clearly identified in the STM images. For this reason, we will focus on the Sb growth in a single domain. Some typical images are shown in Fig. 5; these are clipped from larger scans to show details. The images are arranged in pairs of three. Each pair in a given row approximately represents the same area of the sample imaged and corresponds to the same coverage but different bias voltage. Each image covers an approximate area of 30×30 Å^2 in Figs. 5(a) and 5(b), and 50×50 Å^2 in Figs. 5(c)–5(f). Boxes and circles are drawn, respectively, to indicate the size of the (2×1) unit cell and to highlight specific features as discussed below, but do not represent the same area for a given pair of images.

In Figs. 5(a) and 5(b), a flat region on the clean Si(001)-(2×1) surface exhibiting symmetric dimerization is shown with sample bias voltages of −2.0 and +1.3 V relative to the tip, respectively, to reveal the spatial distribution of the occupied and unoccupied states. In Fig. 5(a), the protrusions (white areas) indicate a pronounced partial density of occupied states situated over the bond joining the two dimer atoms, while the partial density of unoccupied states is seen to maximize at the outer ends of a dimer in Fig. 5(b) corresponding to the locations of the dangling bonds. These results are consistent with previous measurements.[9,20] The neighboring dimers in a row are not resolved under the experimental conditions for these two images.

The images for the 0.3-ML coverage are shown in Figs. 5(c) and 5(d) with sample bias voltages of −2.4 and +2.4 V, respectively. The Sb induces significant disorder. For the positive bias [Fig. 5(d)], the overall (2×1) periodicity can still be recognized, but the original regular dimer-row pattern is now significantly distorted and replaced by a pattern of wavy stripes. Furthermore, the resolved dimer dangling bonds seen in Fig. 5(b) are no longer resolved. It is observed from large-area scans that all parts of the surface are affected by the Sb adsorption at this coverage; thus, the Sb does not form ordered islands or clusters. The Sb-induced disorder is more pronounced in the negative-bias image, Fig. 5(c), where a number of "bumps" and deep "holes" are seen. A typical bump is indicated by the circle in Fig. 5(c). Over a large area, the bumps all appear similar. In between the randomly dis-

tributed bumps and deep holes, however, one can clearly see dimerlike structures; examples can be found near the outlined box for the (2×1) unit cell. The previously unresolved dimer structure is now replaced by two resolved protrusions. Clearly, the dimer electronic structure has been modified by the Sb adsorption, resulting in the "switch" between the appearances of the dimers (namely, the unresolved dimer becomes resolved for the negative bias, while the resolved dimer becomes unresolved for the positive bias after Sb adsorption). Thus, the spatial distributions of the electronic states become transposed after Sb adsorption, with the occupied and unoccupied states now imaged by tunneling at the sides and centers, respectively, of a dimer row. A similar effect has been observed for the dissociative chemisorption of NH_3 on Si(001).[20]

The disorder becomes more severe for increasing Sb coverages. The image for the saturation coverage in Fig. 5(f), with a sample bias of $+2.8$ V, still shows an indication of a (2×1) periodicity in the form of wavy and highly distorted stripes. An attempt to image the occupied states of this same region with negative bias voltages showed only disorder, as seen in Fig. 5(e) taken with a sample bias of -2.5 V. Viewed over a large area, the negative-bias images give the impression of randomly distributed bumps covering the entire surface. A typical bump is indicated by the circle in Fig. 5(e).

3. *Discussion*

The photoemission results indicate the saturation of the Si dimer dangling bond by the adsorption of Sb. The persistence of the (2×1) reconstruction up to the saturation coverage, as observed in the HEED patterns and positive-bias STM images, suggests that the dimerization of the Si surface has not been destroyed by the Sb. Therefore, the interaction between the Sb and Si involves mainly the saturation of the dangling bond to form a chemisorption bond. The disorder is most likely a natural consequence of the large 16% difference in the covalent radii between Sb and Si. A densely packed (1×1) or (2×1) Sb overlayer in a plane would cause too much compression of the Sb atoms. In sharp contrast, the As/Si(001) system is known to exhibit a registered (2×1) pattern at 1-ML saturation coverage.[21,22] This is understandable, because the difference in covalent radii is only about 1% between Si and As. The exact atomic bonding geometry between Sb and Si cannot be deduced from the present study, but is likely to involve a variety of vertical and horizontal distortions of the chemisorption bond as well as defects such as misfit dislocations and vacancies to accommodate the large mismatch is size.

Another interesting difference between Sb/Si(001) and As/Si(001) is that the latter system shows a 0.45-eV adsorbate-induced chemical shift in core-level binding energy for the Si surface atoms.[22] As discussed above, the Sb/Si(001) system shows little chemical shift. The difference can be attributed to the much larger electronegativity of As, resulting in a partially ionic bond between As and Si.[23,24] The valence charge transfer from a Si surface atom to the adsorbed As leads to a higher electrostatic potential energy for the core electrons of the Si surface atom, and hence the core-level binding energy is increased relative to the bulk value. The relationship between bond ionicity and core-level chemical shift has been discussed before.[2,25]

The dramatic changes of the appearance of the dimer structure with Sb adsorption in going from Figs. 5(a) to 5(c) and from Figs. 5(b) to 5(d) can be accounted for by the saturation of the dimer dangling bonds. At 0.3-ML coverage, the number of dimer dangling bonds is reduced from the original value of about 0.9 to 0.2 ML (see Fig. 4). Each dimer has two dangling bonds, so the probability for both to be unaffected by Sb at this coverage is only about 5%, assuming a random distribution of the Sb atoms (since the system is disordered). Thus, essentially all dimers are involved in the bonding to Sb, and the resolved dimers seen in Fig. 5(c) are definitely not the original Si dimers. For clean Si(001), the dimer dangling bonds form partial π-bonding orbitals, leading to the pronounced tunneling midway between the two atoms in a dimer for negative-bias conditions [Fig. 5(a)].[9,20,26] The formation of Sb—Si chemisorption bonds should result in a redistribution of the valence-dangling-bond charge from the in-plane π-bonding configuration to an out-of-plane configuration, since Sb is above the surface. Thus, the tunneling through occupied states from the center of the dimer is significantly reduced relative to tunneling from the ends of a dimer. Similarly, the tunneling into the unoccupied states is now seen to maximize at the center of a dimer, since the bond rehybridization removes the partial π-antibonding orbitals situated at the outer ends of an unreacted dimer. Due to the presence of substantial disorder in the STM images, we cannot determine in more detail the bonding configuration. However, the resolved dimers in Fig. 5(c) appear relatively symmetric, suggesting that both dangling bonds for each dimer are involved in bonding to the Sb.

IV. SUMMARY AND CONCLUSIONS

The interaction between adsorbed Sb and Si(001) has been studied by photoemission, STM, and HEED. The Sb adsorption shows a saturation coverage at about 1 ML at 320–370 °C. Photoemission from the Si $2p$ core level indicates that the adsorption causes the saturation of the Si-dimer dangling bonds by Sb. The number of reacted dangling bonds for a given coverage can be determined from the change in the relative surface core-level photoemission intensity, and on the average each Sb adatom is bonded to about three Si surface atoms for coverages below 0.2 ML and to about two Si atoms for coverages between 0.2 and 0.5 ML. Constant-current STM images show that the starting Si(001) surface consisted of dimerized domains with widely varying sizes separated by atomic steps. A defect density of a few percent in large domains appears to be typical. Sb adsorption does not lead to ordered islands or clusters. The spatial distributions of the occupied and unoccupied electronic states, revealed by taking STM images with negative and positive sample biases, respectively, show interesting changes upon Sb adsorption, in addition to disorder. These changes can be understood in terms of the bond forma-

tion between the Sb and Si. The STM images and HEED patterns also reveal the persistence of the overall (2×1) structure up to the saturation coverage, implying the persistence of the dimerization.

ACKNOWLEDGMENTS

This material is based upon work supported by the U.S. Department of Energy (Division of Materials Sciences, Office of Basic Energy Sciences), under Contract No. DE-AC02-76ER01198. Some of the personnel and equipment support was also derived from grants from the National Science Foundation (Grant Nos. DMR-83-52083 and DMR-86-14234), the IBM Thomas J. Watson Research Center (Yorktown Heights, NY), and the E. I. du Pont de Nemours and Company (Wilmington, DE). We acknowledge the use of central facilities of the Materials Research Laboratory of the University of Illinois, which was supported by the U. S. Department of Energy (Division of Materials Sciences, Office of Basic Energy Sciences), under Contract No. DE-AC02-76ER01198, and the U.S. National Science Foundation under Contract No. DMR-83-16981.

[1]See, for example, the articles presented in Proceedings of the Second International Conference on Scanning Tunneling Microscopy [J. Vac. Sci. Technol. A **6**, 401 (1988)].

[2]See, for example, T.-C. Chiang, CRC Crit. Rev. Solid State Mater. Sci. **14**, 269 (1988); Mater. Res. Soc. Symp. Proc. **143**, 55 (1989).

[3]O. L. Alerhand, D. Vanderbilt, R. D. Meade, and J. D. Joannopoulos, Phys. Rev. Lett. **61**, 1973 (1988).

[4]K. Pandey, in *Proceedings of the Seventeenth International Conference of the Physics of Semiconductors,* edited by D. J. Chadi and W. A. Harrison (Springer-Verlag, New York, 1985), p. 55.

[5]J. E. Demuth, R. J. Hamers, R. M. Tromp, and M. E. Welland, J. Vac. Sci. Technol. **4**, 1320 (1986); IBM J. Res. Dev. **30**, 396 (1986).

[6]D. A. Reed and G. Ehrlich, Surf. Sci. **151**, 143 (1985).

[7]D. H. Rich, T. Miller, G. E. Franklin, and T.-C. Chiang, Phys. Rev. B **39**, 1438 (1989).

[8]S. A. Barnett, H. F. Winters, and J. E. Greene, Surf. Sci. **165**, 303 (1986).

[9]R. J. Hamers, R. M. Tromp, and J. E. Demuth, Phys. Rev. B **34**, 5343 (1986); Surf. Sci. **181**, 346 (1987).

[10]H. Kroemer, in *Heteroepitaxy on Silicon,* Vol. 6 of *Materials Research Society Symposia Proceedings,* edited by J. C. C. Fan and J. M. Poate (Materials Research Society, Pittsburgh, 1986), p. 3.

[11]D. J. Chadi, Phys. Rev. Lett. **59**, 1691 (1987).

[12]P. E. Wierenga, J. A. Kubby, and J. E. Griffith, Phys. Rev. Lett. **59**, 2169 (1987).

[13]J. E. Griffith, J. A. Kubby, P. E. Wierenga, R. S. Becker, and J. S. Vickers, J. Vac. Sci. Technol. A **6**, 493 (1988).

[14]D. E. Aspnes and J. Ihm, Phys. Rev. Lett. **57**, 3054 (1986).

[15]D. H. Rich, A. Samsavar, T. Miller, H. F. Lin, T.-C. Chiang, J. -E. Sundgren, and J. E. Greene, Phys. Rev. Lett. **58**, 579 (1987).

[16]D. H. Rich, T. Miller, and T.-C. Chiang, Phys. Rev. B **37**, 3124 (1988).

[17]D. H. Rich, T. Miller, A. Samsavar, H. F. Lin, and T.-C. Chiang, Phys. Rev. B **37**, 10 221 (1988).

[18]T. Miller, T. C. Hsieh, and T.-C. Chiang, Phys. Rev. B **33**, 6983 (1986).

[19]A. Samsavar, T. Miller, and T.-C. Chiang, Phys. Rev. B **38**, 9889 (1988).

[20]R. J. Hamers, Ph. Avouris, and F. Bozso, J. Vac. Sci. Technol. A **6**, 508 (1988).

[21]R. S. Becker, J. S. Vickers, and T. Klitsner, Bull. Am. Phys. Soc. **33**, 785 (1988).

[22]R. D. Bringans, M. A. Olmstead, R. I. G. Uhrberg, and R. Z. Bachrach, Phys. Rev. B **36**, 9569 (1987).

[23]Linus Pauling, *The Nature of the Chemical Bond* (Cornell University, Ithaca, NY, 1939).

[24]R. T. Sanderson, *Chemical Bonds and Bond Energy* (Academic, New York, 1971).

[25]J. J. Joyce, M. Grioni, M. del Giudice, M. W. Ruckman, F. Boscherini, and J. H. Weaver, J. Vac. Sci. Technol. A **5**, 2019 (1987).

[26]J. A. Appelbaum, G. A. Baraff, and D. R. Hamann, Phys. Rev. B **14**, 588 (1976).

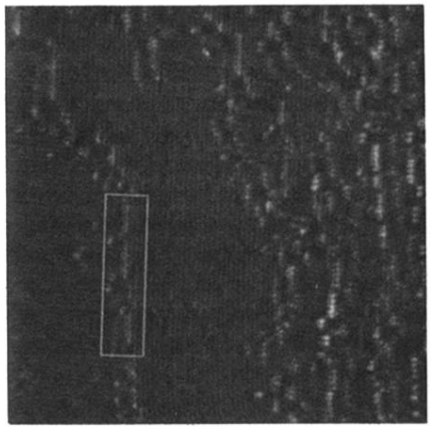

FIG. 1. Constant-current STM image of a 640×640-Å^2 region of clean Si(001)-(2×1) with sample bias of -1.3 V. Examples of S_A- and S_B-type steps are surrounded by white and black rectangles, respectively.

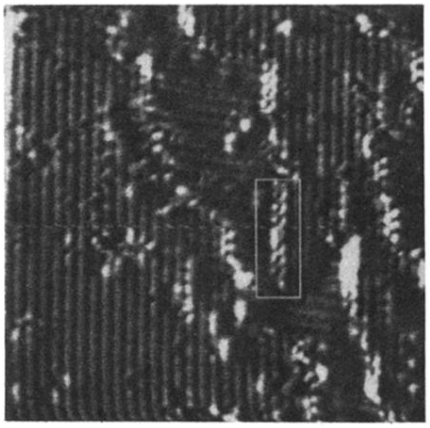

FIG. 2. Constant-current STM image of a 260×260-Å^2 region of clean Si(001)-(2×1) with sample bias of −1.3 V. A white rectangle surrounds an S_A-type step.

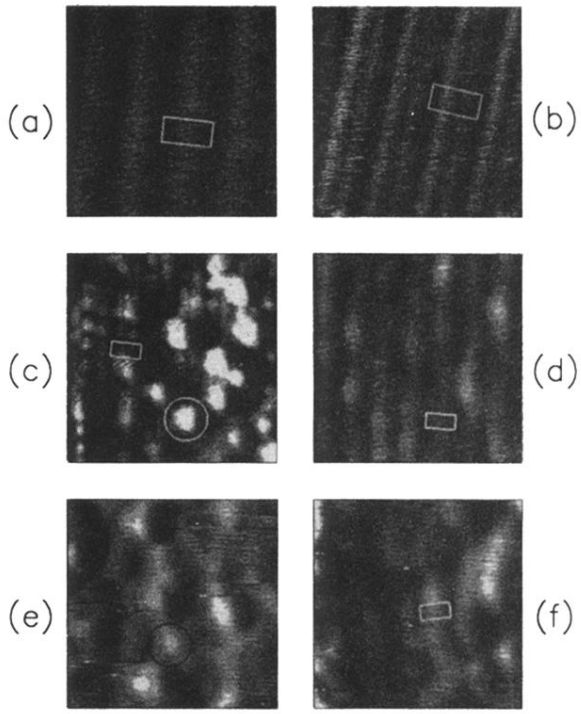

FIG. 5. Constant-current STM images of Si(001) and Sb-covered Si(001). Dark and bright areas represent depressions and protrusions, respectively. The Sb coverages and sample bias voltages are (a) clean, -2.0 V; (b) clean, $+1.3$ V; (c) 0.3 ML, -2.4 V; (d) 0.3 ML, $+2.4$ V; (e) 1 ML, -2.5 V; (f) 1 ML, $+2.8$ V. The rectangles indicate a (2×1) unit cell and circles outline typical bumps due to the Sb-induced disorder.